Fisheries Research 264 (2023) 106720

Contents lists available at ScienceDirect

Fisheries Research

journal homepage: www.elsevier.com/locate/fishres

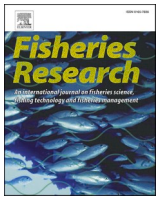

Sound sees more: A comparison of imaging sonars and optical cameras for estimating fish densities at artificial reefs

Edward C.P. Sibley [a,b,*], Travis S. Elsdon [c], Michael J. Marnane [c], Alethea S. Madgett [a], Euan S. Harvey [d], Thomas Cornulier [b,1], Damon Driessen [d], Paul G. Fernandes [b,2]

[a] The National Decommissioning Centre, Newburgh, Aberdeenshire, United Kingdom
[b] School of Biological Sciences, University of Aberdeen, Aberdeen, Aberdeenshire, United Kingdom
[c] Chevron Technical Centre, Perth, WA, Australia
[d] School of Molecular and Life Sciences, Curtin University, Bentley, WA, Australia

ARTICLE INFO

Handled by Andre Eric Punt

Keywords:
Acoustics
Optics
Imaging sonar
Artificial reef
Fishes

ABSTRACT

Imaging sonars are increasingly being utilised in fish surveys in conjunction with or as substitutes for optical instruments. To justify the use of imaging sonars, we must first describe their application, limitations, and efficacy compared to optics. This study compared quantitative data of fish assemblages obtained using imaging sonars operating at four frequencies (0.75, 1.2, 2.1, and 3 MHz) with simultaneous optical camera footage at two artificial reefs. Fish densities were on average three times higher for sonar than optics. Greater detection by the sonar was attributed to site-attached fishes that were camouflaged against the artificial reefs or the adjacent seabed, which could be discriminated by imaging sonar, but not using optics. This suggests that differences in habitat and fish assemblage composition could influence the relative performance and density estimates of imaging sonar versus optics. Several limitations of imaging sonar were identified that need to be accounted for in future survey designs, including: discriminating fishes from benthic growth; an inability to detect fishes within complex habitat structures; and seabed and side-lobe interferences that truncate survey volume. Overall, this study demonstrates the value of imaging sonar for quantifying fish communities and describes limitations and recommendations for their deployment in future surveys.

1. Introduction

Many surveys of the fish biodiversity of tropical and subtropical coastal systems are conducted using optics. Optics assess fishes through visual observation via various platforms, including human-based platforms, such as SCUBA-facilitated Underwater Visual Censuses (UVCs; e.g., Dickens et al., 2011; Samoilys and Carlos, 2000), and remote platforms like camera-mounted Remote Operated Vehicles (ROVs; e.g., Ajemian et al., 2015; Lorance and Trenkel, 2006), and Baited Remote Underwater Videos (BRUVs; e.g., Bond et al., 2012; Dunlop et al., 2015; Willis and Babcock, 2000). Optics can provide high resolution detail of fishes, facilitating their identification and characterising their behaviour, distribution, and community structure (Dunlop et al., 2015; Stoner et al., 2008). However, optics are light-dependent, hence are limited in low visibility scenarios (e.g., at depth, at night, or in turbid water). Optics are also typically characterised by the limited range that visible light can penetrate the water, and are altogether inhibited by opaque physical barriers, ranging from particulates in the water column to artificial structures. As such, the spatial extent of optics is constrained, which limits optic quantification of sparsely distributed and rare species (Ajemian et al., 2015; Tessier et al., 2005), and fishes in large aggregations (Munnelly et al., 2019). Complementary survey techniques that do not share the limitations of optics are, therefore, needed to provide a more complete assessment of fish communities, particularly in areas of restricted visibility.

Active acoustic devices, collectively known as SONAR, function by propagating an acoustic pulse into the water column and detecting echoes which are reflected back from physical objects such as fishes. These echoes can be graphically displayed and, in many cases, enumerated accurately to provide estimates of abundance (Martignac

* Corresponding author at: School of Biological Sciences, University of Aberdeen, Aberdeen, Aberdeenshire, United Kingdom.
E-mail address: e.sibley.20@abdn.ac.uk (E.C.P. Sibley).
[1] Present Address: Biomathematics and Statistics Scotland, Craigiebuckler, Aberdeen, Aberdeenshire, United Kingdom.
[2] Present Address: The Lyell Centre, Herriot Watt University, Edinburgh, United Kingdom.

https://doi.org/10.1016/j.fishres.2023.106720
Received 9 December 2022; Received in revised form 12 April 2023; Accepted 16 April 2023
Available online 23 April 2023

et al., 2015; Mueller et al., 2006), provided the system is calibrated. This can also allow for measurements of distance and object size. Objects are typically compressed from three dimensions to be displayed in two dimensions (Simmons and MacLennan, 2005). Several classes of active acoustic devices are used in marine surveys, including single beam echosounders operating at moderate frequencies (typically 38–420 kHz); and multibeam sonars utilising a broad range of frequencies, from low frequency, long-range fish finding and military sonar (a minimum of around 12 kHz), to high-frequency sonars used to monitor the integrity of subsea industrial infrastructure (up to 3 MHz).

Sound of low to moderate frequency (1–100 s kHz), travels much farther in water than light, enabling acoustics to detect objects significantly beyond visual range, providing greater spatial coverage than optics and permitting effective detection of objects independent of light (Cook et al., 2019; Mueller et al., 2006). However, this comes at the expense of resolution, and although fish size, distribution and density can be readily quantified using acoustics (Boswell et al., 2010), species identification is challenging (Bollinger and Kline, 2017; Egg et al., 2018; MacLennan and Holliday, 1996), including for multibeam sonar (Mueller et al., 2006; Becker et al., 2013). Where light is not limiting, optics can be used to provide information to identify acoustic targets, sometimes known as "groundtruthing" (Bolser et al., 2020; Stanley and Wilson, 2000, 1997), but more accurately termed "additional evidence" (Fernandes et al., 2016). Calibrated stereo-camera systems, comprising two cameras with converging fields-of-view, can provide additional information on object position, and therefore size, that cannot be acquired using single cameras (Harvey et al., 2002).

The resolution of the sonar device can be improved by increasing the frequency of the acoustic pulse. Though this is offset by a decrease in range, the resulting increase in resolution can provide near optic-quality snapshots of fish assemblages that are comparable to ultrasound images generated in diagnostic radiology. In the last two decades, very high frequency sonars, known as imaging sonars or acoustic cameras (hereafter referred to as imaging sonars), have proliferated in the study of fishes and their behaviour. Comprised of multiple beams transmitted from around 0.7–3 megahertz (MHz), imaging sonars generate continuous sequences of monochrome acoustic images that can capture multiple fish metrics including abundance (Able et al., 2013; Becker et al., 2016, 2013, 2011; Capoccioni et al., 2019); size (Able et al., 2013; Becker et al., 2013; Lankowicz et al., 2020; Rodriguez-Pinto et al., 2022; Van Hal et al., 2017; Viehman and Zydlewski, 2015); various behavioural attributes, including swim pattern (Becker et al., 2013), schooling behaviour (Capoccioni et al., 2019; Lankowicz et al., 2020; Viehman and Zydlewski, 2015), habitat associations (Grabowski et al., 2012; Mueller et al., 2006), reproduction (Grabowski et al., 2012; Langkau et al., 2016), predation (Becker and Suthers, 2014; Handegard et al., 2012; Rieucau et al., 2016), and migration (e.g., Brehmer et al., 2006; Egg et al., 2017; Faulkner and Maxwell, 2020); ecological group assignations (Able et al., 2013); and combinations of the above (Able et al., 2013).

Imaging sonars have been used extensively to quantify fishes around various artificial habitats, such as piers (Able et al., 2013; Shahrestani et al., 2017), renewable energy infrastructure (Egg et al., 2017; Mour-sund et al., 2003; Van Hal et al., 2017; Viehman and Zydlewski, 2015), levees (Eggleston et al., 2020), and rigs-to-reefs (Plumlee et al., 2020). To determine the effectiveness of imaging sonars in enumerating fishes relative to optics, direct comparisons between the two instrument types are needed, particularly to establish the potential of imaging sonar as a substitute for optics in low-light conditions. Previous comparisons of imaging sonar versus alternative optical methods for quantifying fish abundance have yielded mixed results. One example compared counts of sockeye salmon passing through an enumeration fence using a Dual-frequency IDentification SONar (DIDSON) with visual counts, finding strong agreement between the two methods (Holmes et al., 2006). In that case, however, the sampling volume was constrained and fish abundance was high. Alternatively, (Egg et al., 2018) reported higher detection rates of fishes in a shallow river than a high-definition (HD) camera. Overall, comparisons in non-riverine habitats and for multi-species assemblages are needed to evaluate the capacity of imaging sonars to enumerate fishes in ecosystems such as reefs.

This study conducted simultaneous imaging sonar and optic surveys of the fish assemblages around two artificial reefs, the Rottnest fish towers, off Perth, Western Australia. The towers are situated in the flow of the Leeuwin current, which brings tropical water from the north to mix with the temperate water of the south. As a result, the marine fauna of the region is a diverse blend of tropical and temperate taxa (Hutchins and Pearce, 1994). This study determined the distinctive sampling volumes of both instruments to estimate fish density (number per cubic metre). The specific objectives were to: 1) quantify the ability of imaging sonar to enumerate fish densities relative to optics across a range of frequencies, and 2) identify the key limitations of imaging sonar through comparison with optics. The overall aim of the study was to improve our understanding of the performance of imaging sonar and its efficacy as a standalone or complementary tool to enumerate fish assemblages.

2. Methods

2.1. Study site

The Rottnest fish towers are two steel artificial reefs situated on the outer continental shelf of Western Australia, 11 km south of Rottnest Island and 27 km west of Perth (Fig. 1). The towers are approximately 150 m apart, with the north tower situated at − 32° 07'.461 S, 115° 26'.978 E (45 m deep) and the south tower at − 32° 07'.527 S, 115° 27'.013 E (44.3 m deep). Deployed in 2017 by SubCon (www.subcon.com) to act as fish aggregating devices and bolster commercial fisheries, the towers are 12.5 m tall, 10 m long and 7.8 m wide (Fig. 1) and are positioned on unconsolidated soft sediment. Sampling took place on 28th September 2021 during daylight hours (09:30–15:00). Tide height varied by approximately 1.8 m during this period, with a high of 2.21 m at 08:52, and a low of 0.42 m at 17:29. Visibility was estimated at 15–25 m throughout the study.

2.2. Instruments

Fishes were acoustically detected using imaging sonars mounted on an Oceanbotics SRV-8 Remotely Operated Vehicle (ROV) (www.oceanbotics.com/srv-8). Three Blueprint Subsea Oculus multibeam imaging sonars (the M750d, M1200d, and M3000d; Table 1) that encompassed the general range of frequencies used by imaging sonar were deployed interchangeably, each capable of operating at two different frequencies (i.e., dual frequency). Increasing the frequency of imaging sonars improves the resolution of detected targets, at the cost of reduced range and, subsequently, sampling volume. The north tower was surveyed at 3 MHz with the M3000d, and the south tower was surveyed at 0.75 MHz (M750d), 1.2 MHz, and 2.1 MHz (both M1200d). Due to unfavourable weather conditions prior to surveying the north tower at 0.75, 1.2, and 2.1 MHz and the south tower at 3 MHz that prevented ROV deployment, this study could not survey both towers across all frequencies. Range was restricted to 5 m at 3 MHz and set to 10 m for the remaining three frequencies.

The optic system consisted of the integrated dual-mode HD camera onboard the ROV. The camera was situated behind a dome port and recorded video at 1080 p (30 fps). The ROV was pitched and tilted as orthogonally as possible. The vertical aperture of the camera field of view (FOV) was 65.4°, with a horizontal aperture of 99.1°. The imaging sonars were mounted atop the ROV, in the same vertical plane as the onboard camera (Supplementary Fig. 1). The ROV was tethered to the surface via an umbilical, and an Ultra-short Baseline (USBL) Positioning System was fitted to the ROV determine its location. The ROV also housed a depth meter.

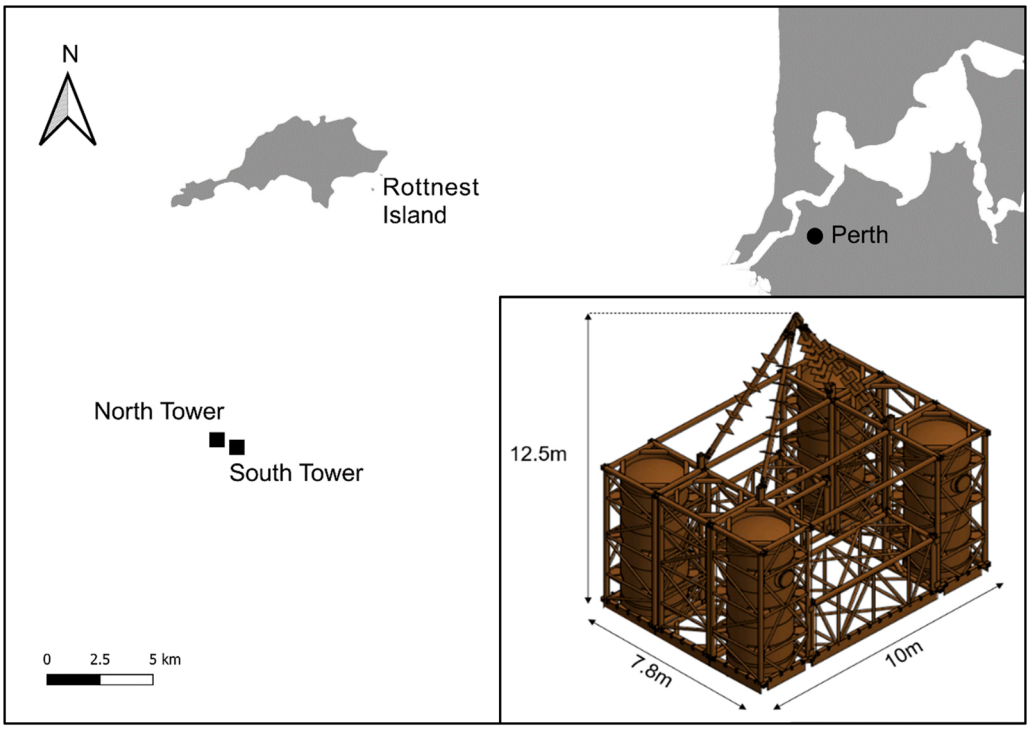

Fig. 1. Map of the study site, the north and south Rottnest fish towers, south of Rottnest Island and southwest of Perth, Western Australia. Inset: schematic of the towers, which are identical in structure.

Table 1
Specifications of the three Blueprint Subsea Oculus multibeam imaging sonars used in this study.

Model	M750d		M1200d		M3000d	
Frequency (MHz)	0.75	1.2	1.2	2.1	1.2	3
Max. Range (m)	120	40	40	10	30	5
Range Resolution (mm)	4	2.5	2.5		2.5	2
Horizontal Aperture	130°		130°	60°	130°	40°
Vertical Aperture	20°		20°	12°	20°	
Max. Number of Beams	512		512		512	
Angular Resolution	1°	0.6°	0.6°	0.4°	0.6°	0.4°
Beam Separation	0.25°		0.25°	0.16°	0.25°	0.1°

2.3. Survey design

The towers comprise three conspicuous depth strata: the lower strata (the base of the towers, from the seabed to approximately 3 m above the seabed), the upper strata (the top of the towers, between approximately 3–6 m above the seabed), and the spire (the pyramidal structure atop the towers, between approximately 6 and 12.5 m above the seabed, Fig. 1). At the lower and upper strata, sampling was conducted by holding the ROV stationary for twenty seconds at four sampling stations that collectively encompassed the entire periphery of the towers at both strata: at the middle of each of the length-ward and width-ward sides of the tower facing inward. Twenty seconds was chosen as the sampling duration at each station to generate sufficient footage for analyses whilst minimising the challenge of holding the ROV steady in instances of strong current. Furthermore, no adverse impacts of the ROV on fish behaviour, such as avoidance or attraction, were observed, so no acclimation time was incorporated into the sampling duration. To maintain a consistent sampling volume, the ROV was held as stationary as possible at each sampling station, between 1.42 and 2.75 m away from the structure as determined using the distance gradings on the Oculus Viewpoint display (www.blueprintsubsea.com/oculus/support.php). At the spire, continuous point-count transects were conducted by flying the ROV up one leg of the spire to the apex, then down the adjacent leg to the intersection of the spire and the upper stratum.

2.4. Data processing

The twenty second intervals of continuous optic and imaging sonar footage taken at each sampling station in the lower and upper strata were partitioned into five still frames taken every five seconds. This generated twenty still frames per instrument (including twenty still frames per imaging sonar frequency) across all sampling stations per stratum. All fishes present in each frame per instrument were counted manually by one observer (E.C.P. Sibley) to avoid the possibility of inter-observer variation in counts (Jones et al., 2021; Keefer et al., 2017). For both imaging sonar and optic still frames, only fishes that were fully in the FOV were counted. Consecutive still frames were used to discriminate and subsequently count individual fishes in instances of high fish density, such as schooling, where fishes were occasionally obscured from detection by other individuals. This was done independently for each instrument (i.e., optical footage was not used to help resolve the number of fishes on the simultaneous imaging sonar display, and vice versa). To avoid the challenge of manually tracking individual fishes over sequences of continuous footage, fishes were counted in still frames from each sampling station, mitigating the risk of multipassing. Multipassing occurs when the same fish exits and re-enters the FOV in continuous sequences of footage, and is therefore counted twice in the same sampling interval, causing overestimation in fish abundance (Shahrestani et al., 2017; Viehman and Zydlewski, 2015). The number of fishes in each frame was counted only once, with the count of fishes from each frame per instrument used as a metric of fish abundance.

Preliminary inspection of the imaging sonar and simultaneous optic still frames showed the upper strata and spires of both towers to be densely colonised by protruding soft corals, sponges, and algae. Fishes occupying the upper strata and spires could not be consistently discriminated from benthic growth using imaging sonar, and fishes in close proximity to the towers were frequently obstructed from sonar detection by extensive benthic growth (Fig. 2a). The 0.75 and 1.2 MHz

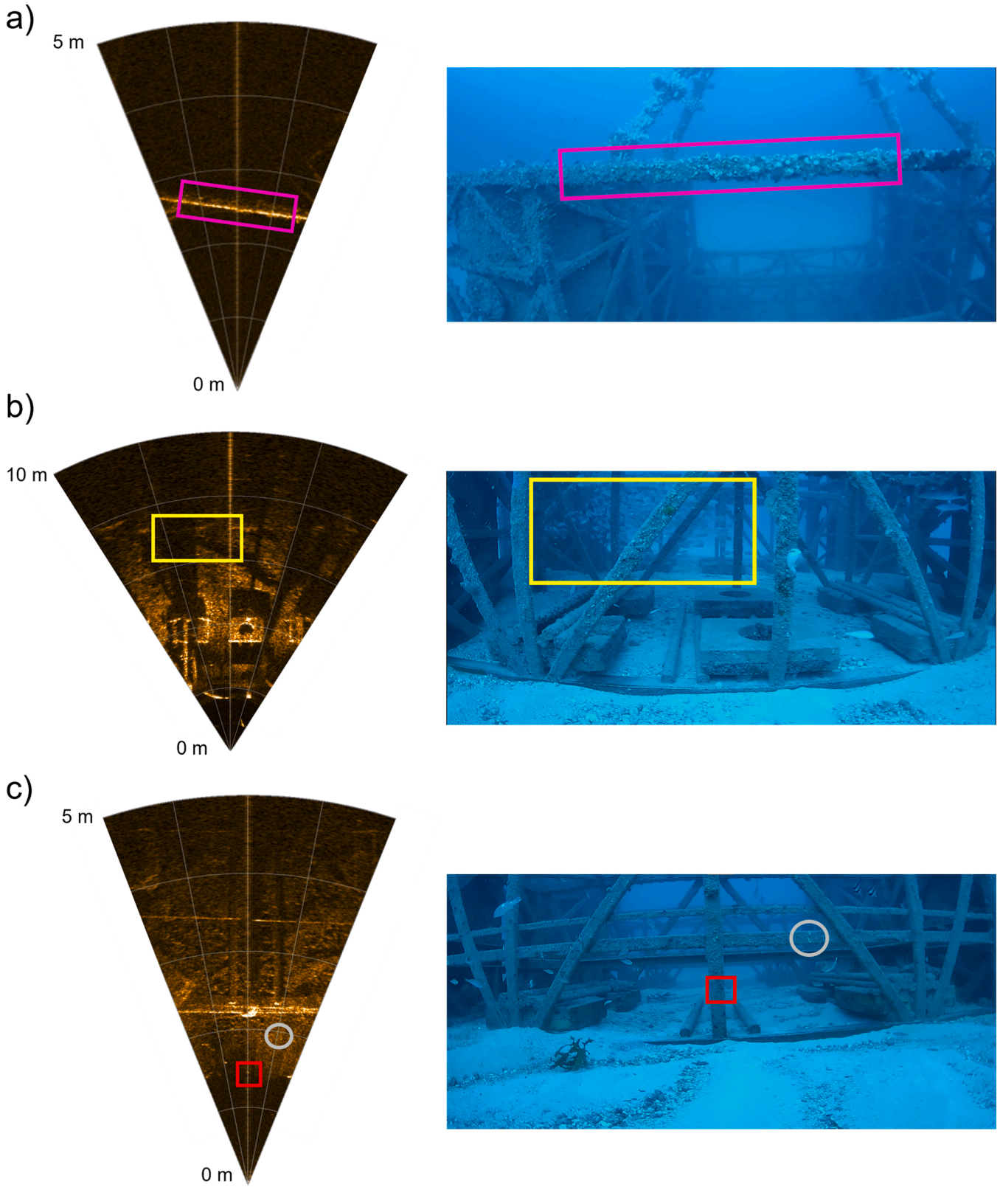

(caption on next page)

Fig. 2. Imaging sonar still frames and corresponding optic still frames demonstrating the key limitations of imaging sonar for quantifying fishes on artificial reefs of high structural complexity: a) the challenges of discriminating fishes from benthic growth. As shown here, benthic growth can appear as fish scatter (encompassed by the pink rectangle on the sonar image), yet contemporaneous optics reveal the true absence of fishes (the approximately corresponding region on the optical image is indicated by the pink rectangle); b) failure to detect fishes occupying the interstitial space of the Rottnest fish towers due to masking by the physical structure of the towers themselves. In this instance, a school of goldlined seabream (*Rhabdosargus sarba*) are clearly visible in the optic still frame occupying the back left (yellow rectangle) of the interstitial space of the tower respectively. However, these fishes are not present in the corresponding imaging sonar still frame (echoes would otherwise appear approximately in the yellow rectangle on the sonar image); c) in several instances, downward pitching of the ROV complex resulted in the seabed being ensonified prior to the towers. This may mask fishes: in this example at 3 MHz, the fishes detected in the imaging sonar still frame (mostly West Australian pullers, *Chromis westaustralis*, as evidenced by the simultaneous optics) are challenging to distinguish from the seabed (which appears as intense backscatter starting from ~1.4 m to the tower). Two *C. westaustralis* (circled in grey) are visible on the optical image but are masked by the seabed on the imaging sonar frame (they would otherwise appear approximately within the grey circle on the sonar image). Note also the fish detected in the sonar image encompassed by the red rectangle – this is not visible in the simultaneous camera image (it would otherwise be present approximately within the red rectangle), and is likely a *C. westaustralis* that is camouflaged against the structure.

frequencies particularly lacked the resolution to distinguish these fishes from benthic growth. This study was therefore restricted to quantifying fishes in the lower depth strata of the towers, where benthic growth was sparser. Preliminary inspection also revealed that fishes occupying the interstitial space of the towers were obstructed from detection by the physical structure of the towers themselves (Fig. 2b). Fishes were also occasionally masked by the substrate, in instances where the ROV complex was pitched downwards, resulting in the imaging sonar beam array intercepting the substrate before the towers (Fig. 2c). Also, the towers generated side-lobe interference in the imaging sonar beam array, whereby interception of the dense physical structure of the tower by one beam in the array interferes with adjacent beams. This generated a 'noise-free zone' between the sonar and the towers, in which fishes could be clearly detected, but masked fishes located beyond the zone from detection (Fig. 3). Counts of fishes for both the imaging sonar and optic still frames were, therefore, restricted to the 'noise-free zone' outside of the towers at the lower strata.

Following Han and Uye (2009), fishes in the near-field zone of the imaging sonar (estimated at 0.5 m) were not counted, as targets are often undetectable at close ranges. To calculate the volume of water ensonified by the imaging sonar, the shape of the beam array was determined to be a rectangular-faced segment of a sphere with a base that tapered to the apex of the beam array (further details in Supplementary Material and Fig. S2), with the volume of water ensonified by the imaging sonar calculated as:

$$V_a = \frac{2}{3} \times \beta \times r^3 \times \sin\left(\frac{\alpha}{2}\right) \quad (1)$$

where: β = vertical aperture (expressed in radians); r = distance from the sonar face to the nearest point of the structure (i.e., the radius of the noise-free zone); and α = horizontal aperture (radians). The volume of the near-field zone ($r = 0.5$ m) was then subtracted from this volume to calculate the volume of the noise-free zone in which fishes could be reliably detected. This formula and assumed imaging sonar beam array shape represents an advance on previous studies that assumed more rudimentary beam shapes (e.g., truncated rectangle-based pyramid in Han and Uye, 2009; Lankowicz et al., 2020; Shahrestani et al., 2017). Rectangle-based pyramids are instead appropriate for calculating the volume of optical cameras when the FOV is constrained by a physical structure. Here, the 'base' of the camera FOV comprised the planar exterior of the towers themselves. Both fish counts and distance from the sonar face to the tower were determined using the Oculus Viewpoint display.

For the optic still frames, all fishes were counted and identified to species level using RJE SubNav software (v1.2.38; www.oceanbotics.com/sub-nav), which allows the user to watch footage from the on-board camera of the SRV-8 and log observations both in real-time and retrospectively. The identity of fishes was ascertained in order to determine the relative abundance of each fish species at the study site. This could then inform the relative capacity of each instrument to detect reef fishes based on the taxonomic composition of the assemblage. Where identification was challenging, adjacent frames were used to determine species identity. The sampling volume of the camera was assumed to be a rectangle-based pyramid, with the formula:

$$V_o = \frac{h \times w \times d}{3} \quad (2)$$

where h is the height of the still frame, w is the width of the still frame, and d is the depth of the optical camera FOV, proxied as the distance between the ROV complex and the tower. The height and width of the still frame were determined using discrete structural features of the

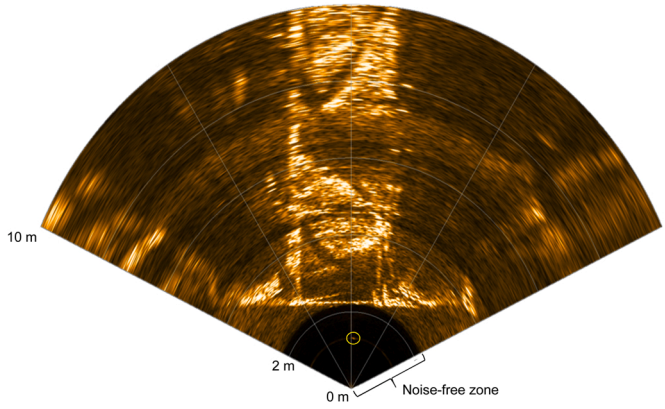

Fig. 3. Side-lobe interference in the imaging sonar beam array at 0.75 MHz that generates a hemispherical noise-free zone commensurate with the distance from the imaging sonar to the structure, in which fishes (such as the one in the centre of the beam array at 1.25 m range, circled in yellow) can be clearly detected. Beyond the zone, however, the interference is too strong to detect fishes. Side-lobe interference occurs across all frequencies.

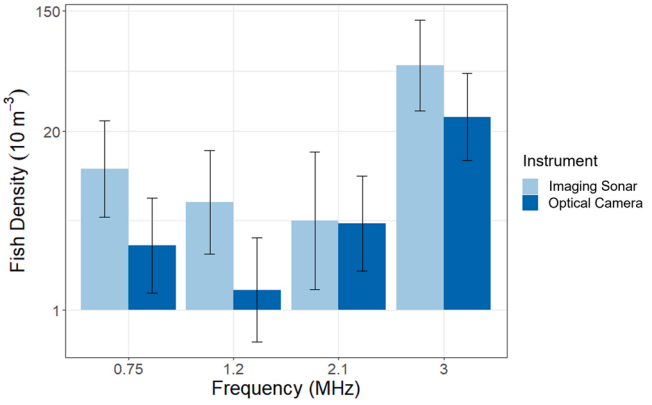

Fig. 4. Fish densities quantified using optics and ensonified across all four frequencies of imaging sonar used at the north and south Rottnest fish towers in this study. Error bars show 95% confidence intervals. Note the logarithmic scale on the y-axis, indicating that similar differences in heights of the bars correspond to similar density detection ratios.

towers that were visible in the frame, such as crossbars and the pillars that comprised the legs of the towers (see McLean et al., 2018). The distances in both height and width between these features were determined through comparison with scaled schematics of the towers. In frames that included the seabed, the volume obscured by the seabed was estimated and subtracted from the total volume of the frame. Visual inspection of fish densities across imaging sonar frames showed no reduction in fish densities in frames with seabed interference, so the volume of the seabed that was ensonified in these frames was not calculated nor subtracted from the total sampling volume of the imaging sonar.

Count data (X) from imaging sonar and optic sampling intervals (time frames, t) were paired and thus non-independent. To accommodate these properties a Generalised Additive Mixed Model (GAMM) was fitted to the data to determine the effect of instrument and imaging sonar frequency on fish density, assuming a negative binomial distribution with dispersion θ, of the form:

$$X_{i,t} \sim NegBin\left(\lambda_{i,t}, \theta\right) \tag{3}$$

$$\ln(\lambda_{i,t}) = \ln(V_i) + \alpha_{i,f} + \gamma_s + \omega_{s,t} + \varepsilon_s \tag{4}$$

where the term $\alpha_{i,f}$ represents the interaction of instrument i (imaging sonar or optical camera) and frequency f; the first order autoregressive term $\omega_{s,t} = \phi\omega_{s,t-1}$; and γ_s and ε_s are random effects of sampling stations s and time frames t within station s, accounting for variation in fish counts between stations and time frames respectively. The natural logarithm of sampling volume for each instrument per observation $\ln(V_i)$ was specified as an offset to constrain the model to treat the dependent variable as density (number of fishes per unit volume). Density was modelled for both the imaging sonar and the optical camera instead of raw abundances due to the difference in sampling volume between the instruments. The significance of the respective effects of instrument, frequency, and the interaction between instrument and frequency was determined through Analysis of Deviance with F-tests. Statistical significance was determined at the threshold of $p < 0.05$. All statistical analyses were conducted in R (Team, 2013), and the model fitted using the 'gamm' function in the package "mgcv" (Wood and Wood, 2015), using treatment contrasts.

3. Results

3.1. Imaging sonar and optic fish densities

The fish densities detected by the imaging sonar and optical camera followed similar trends, but were higher for the sonar at 0.75, 1.2, and 3 MHz (Fig. 4). Density estimated by the sonar was on average 3.014 times higher than optics (means with standard errors: 3.622± 0.236, 4.339 ±35.354, 1.053 ±1.625, and 2.356 ±3.982 higher at 0.75, 1.2, 2.1 and 3 MHz respectively). Analysis of deviance of the GAMM revealed a significant effect of imaging sonar frequency, instrument type (imaging sonar or optical camera), and the interaction between frequency and instrument type on fish density (frequency – df = 3, F = 9.692, p = 6.83 $\times 10^{-6}$; instrument – df = 1, F = 29.642, p = 2.04 $\times 10^{-7}$; frequency:instrument – df = 3, F = 2.861, p = 0.039). Summary coefficients for the GAMM components are presented in Supplementary Table 1. Visual inspection of fish density estimates and confidence intervals in Fig. 4 suggested that the effect of instrument was primarily driven by differences between the imaging sonar and optical camera at 0.75, 1.2, and 3 MHz; a lack of overlap between 95% confidence intervals of the sonar densities and the mean of the optic densities at these frequencies indicated that these differences were significant. Minimal difference in estimated fish density at 2.1 MHz suggested a weak or no effect of instrument at that frequency, although confidence intervals were particularly wide, suggesting high variability in observations. The significant effect of frequency was likely to be largely driven by overall higher fish densities recorded by both imaging sonar and optical camera at 3 MHz. This is attributable to a higher fish density at the north Rottnest fish tower (site of the 3 MHz survey), with respect to the south tower (site of the 0.75, 1.2, and 2.1 MHz surveys). The first order autoregressive coefficient was estimated to be $\phi = 0.216$. Respective standard deviations (sd) of the random effects of time frames (6.033×10^{-5}) and sampling station (1.160) suggested that most of the variation in fish densities occurred between sampling stations.

Table 2
Total counts and percentage contribution of all species (n = 13) recorded on optic still images. Counts of each species corresponding to the frequency of the simultaneous imaging sonar used are also presented, used to determine the proportion of each species present when sampling with each frequency.

Species	Frequency (MHz)	Count	Percentage Contribution
Bodianus frenchii	0.75	0	0.000
	1.2	0	0.000
	2.1	0	0.000
	3	3	0.829
Choerodon rubescens	0.75	1	1.176
	1.2	0	0.000
	2.1	0	0.000
	3	0	0.000
Chromis westaustralis	0.75	53	62.353
	1.2	10	37.037
	2.1	39	54.167
	3	269	74.309
Coris auricularis	0.75	24	28.235
	1.2	16	59.259
	2.1	29	40.278
	3	77	21.271
Eubalichthys cyanoura	0.75	2	2.353
	1.2	0	0.000
	2.1	0	0.000
	3	0	0.000
Eubalichthys mosaicus	0.75	1	1.176
	1.2	0	0.000
	2.1	0	0.000
	3	0	0.000
Labroides dimidiatus	0.75	0	0.000
	1.2	0	0.000
	2.1	0	0.000
	3	1	0.276
Neatypus obliquus	0.75	2	2.353
	1.2	0	0.000
	2.1	1	1.389
	3	0	0.000
Parupeneus chrysopleuron	0.75	2	2.353
	1.2	0	0.000
	2.1	0	0.000
	3	0	0.000
Pseudocaranx georgianus	0.75	0	0.000
	1.2	1	3.704
	2.1	1	1.389
	3	0	0.000
Pseudolabrus biserialis	0.75	0	0.000
	1.2	0	0.000
	2.1	2	2.778
	3	0	0.000
Scorpis georgiana	0.75	0	0.000
	1.2	0	0.000
	2.1	0	0.000
	3	1	0.276
Trachinops brauni	0.75	0	0.000
	1.2	0	0.000
	2.1	0	0.000
	3	11	3.039

3.2. Fish assemblage composition

A total of 546 fishes from 13 species were recorded on optic still images at the Rottnest fish towers. Across all frequencies, the most abundant species was West Australian puller (*Chromis westaustralis*), comprising 67.949% of all fishes; followed by western king wrasse (*Coris*

Table 3
Description of the challenges, implications, and potential solutions associated with the limitations of imaging sonar demonstrated and discussed in this study.

Limitation	Challenge	Implication for Assessments and Interpretation	Possible Solutions
Lack of spectral resolution	Colour-based discrimination (e.g., species identification) is very limited even for high-frequency imaging sonars	Imaging sonar assessments of fish assemblages are often restricted to metrics that are quantifiable independent of spectral resolution (e.g., abundance)	Gathering "alternative evidence" for factors like species identification, such as simultaneous optic surveys.
Limited dynamic range	Acoustic scatter from fish and non-fish objects, like soft benthic taxa (e.g., soft corals, sponges), can be difficult to apportion	Fish and non-fish objects may not be discriminable (e.g., benthic, site-attached fishes are likely to be underestimated by imaging sonar at habitats with profuse benthic growth)	Thresholding the sonar echoes to only include high-intensity fish scatter may reduce target obstruction by lower-density objects (e.g., soft corals, sponges), whilst concurrent use of optics could discriminate fishes from high-density targets (e.g., scleractinian corals).
Physical interferences	Side-lobe interference: when one beam in the sonar array intercepts a dense object, side lobes from adjacent beams may also detect that object, creating noise in those adjacent beams at range	Sampling volume around architecturally complex and structurally dense habitats is constrained	Deploying sonar at greater ranges from the habitat to reduce the proportion of side-lobe interference within the sampling volume.
	Structural interference: when dense physical objects (e.g., the steel crossbars of the Rottnest fish towers) prevent beam penetration, obscuring fishes behind the objects from detection	Detection of fishes occupying interstitial refugia within complex habitats is limited	Using optic instruments to survey interstitial fishes, and orienting and/or moving the sonar in and around the interfering objects.
Near-field zone	At very short ranges (usually <0.5 m), the sonar beam array is still forming, so any objects within that range are not fully ensonified	Targets within the near-field zone may appear differently to objects at greater ranges (e.g., less detailed), or not at all	Increasing the range of the sonar from the target habitat to account for the near-field zone, or use optics to quantify fishes in close proximity to the sonar.
High frequency geometric scattering	Fish body parts of varying density scatter high frequency and narrow acoustic beams differently, often resulting in segmentation within an individual fish that appears as multiple targets	Counts of targets may be overestimated	Employ a data processer experienced in identifying geometric scattering, as well as use of an optic instrument and continuous sonar footage to confirm the presence and number of individual targets where possible.
Seabed masking	Ensonification of the seabed (a high-density object) can obscure targets between the sonar and the seabed	Targets near the seabed, or targets detected when the sonar is pitched toward the seabed, may be underestimated	Ensure the sonar is not ensonifying the seabed prior to sampling, or use an optic instrument for surveying targets in instances of seabed masking.
Dimensional compression	Acoustic targets in 3-D space (horizontal, X; vertical, Y; range, Z) are displayed in two-dimensional space	Targets in the same Y plane may obscure one another on acoustic displays	Calibrated stereo-camera systems that provide information of fish arrangement in 3-D space may be used, however these cannot discriminate fishes in the same Z plane.

auricularis, 26.740%); bluelined hulafish (*Trachinops brauni*, 2.015%); western footballer (*Neatypus obliquus*) and foxfish (*Bodianus frenchii*) (both 0.549%); redband wrasse (*Pseudolabrus biserialis*), silver trevally (*Pseudocaranx georgianus*), yellow striped goatfish (*Parupeneus chrysopleuron*), and bluetail leatherjacket (*Eubalichthys cyanoura*) (all 0.366%); and baldchin groper (*Choerodon rubescens*), bluestreak cleaner wrasse (*Labroides dimidiatus*), banded sweep (*Scorpis georgiana*), and mosaic leatherjacket (*Eubalichthys mosaicus*) (all 0.183%). Proportions of each species at each frequency are displayed in Table 2.

4. Discussion

This study provides one of the first comparisons between imaging sonar and optics in surveying fish assemblages in complex habitats. There was a significant effect of instrument type (imaging sonar or optical camera) on recorded fish densities, with the greatest differences in densities occurring at 0.75, 1.2 and 3 MHz, where sonar density was higher than optic density. This study also reports a significant effect of frequency; fish density was likely much higher at the north tower, where only 3 MHz was used, therefore it was not possible to distinguish the effect of local density versus frequency. However, this did not prevent us from estimating the difference in detection rates between the two instruments at this frequency, which was comparable to that observed at 0.75 and 1.2 MHz. The higher densities quantified by imaging sonar in this study conform with reports of imaging sonar quantifying higher fish densities than optical methods (Accola et al., 2022; Egg et al., 2018). This study reinforces these findings by providing a comparison between imaging sonar and optics for a more speciose fish assemblage in a deeper habitat, and as such is more broadly appropriate for inferring the relative performance of imaging sonar to quantify fishes in diverse marine ecosystems.

4.1. Limitations of imaging sonar

In addition to the general, extensively described drawbacks of acoustics (e.g., limited resolution for species identification – Bollinger and Kline, 2017; Egg et al., 2018; MacLennan and Holliday, 1996), this study has identified several key limitations of imaging sonar that compromise its effectiveness for surveying fishes around complex, hard substrate habitat (Table 3). Preliminary inspection of the imaging sonar footage revealed that imaging sonar consistently failed to distinguish fishes from soft benthic growth of medium and high complexity (e.g., sponges, and soft corals, respectively; as determined using simultaneous optical footage), even when inspecting consecutive sequences of footage. This restricted analyses to footage collected from the deeper strata of the Rottnest fish towers where benthic growth was sparser, limiting imaging sonar application for fish surveys on heterogeneous habitats such as coral reefs. Thresholding of the echo to only include

high-intensity fish scatter, as commonly practiced using lower-frequency acoustic instruments (e.g., echosounders), may reduce the masking of fishes by benthic growth (Lankowicz et al., 2020). However, this is unlikely to prove effective for high-density benthic growth (e.g., scleractinian corals). This study recommends that contemporaneous optic footage be used to distinguish fishes from benthic growth using visual characteristics such as colour where necessary, provided visibility is adequate. Continuous imaging sonar footage may also be used to discriminate fishes from benthic growth, but this is challenging if the fishes do not exhibit active behaviour (Artero et al., 2021; Staines et al., 2022). Nevertheless, the consistent detection of benthic growth in this study corroborates the use of imaging sonars to profile heterogeneous biogenic habitats (Griffin et al., 2020).

The imaging sonar used in this study consistently failed across all four frequencies to detect fishes occupying the interstitial waters of the towers. The size and structural complexity of the towers generate ample sheltered interstitial space occupied by a diversity of fishes. However, the assorted crossbars that border the interstitial space are strong reflectors of the acoustic beam array, inhibiting beam penetration, hence preventing the detection of interstitial fishes. Nevertheless, in contrast to Van Hal et al. (2017), this study found no evidence of masking of fishes in close proximity to structure by backscatter from the structure itself, further indicating that imaging sonars are suitable for quantifying site-attached fishes, provided there is no structural obstruction between the sonar and the targets. Furthermore, the degree of structural interference for both interstitial and peripheral fishes is likely less apparent for artificial habitats that are less structurally complex than the Rottnest fish towers, such as wind turbine monopiles (Van Hal et al., 2017) and piers (Able et al., 2013; Accola et al., 2022).

Across all four frequencies, interception of the beam array by the physical structure of the towers generated strong side-lobe interference. This produced a hemispherical 'noise-free void' with a radius equal to the distance between the sonar and the nearest point of the structure, in which targets could be easily identified. Beyond the void, interference was too strong for target detection. This phenomenon was strongest at the two lowest frequencies: 0.75 and 1.2 MHz, a finding in contrast to Cotter and Polagye (2020) who reported stronger side-lobe interference at higher frequencies. This discrepancy may be due to differences in the type of marine habitat surveyed, particularly the density and complexity of the habitat physical structure, though further investigation as to the drivers of side-lobe interferences is warranted. The volume in which fishes can be detected by imaging sonar is further reduced by the near-field zone (around 0.5 m – Han and Uye, 2009), in which objects cannot be consistently detected as the beam array is still forming within these ranges. Future imaging sonar studies may look to define survey volume commensurate with the radius of the noise-free void and near-field zone. Here, deploying the ROV at further distances from the towers would increase the range of the sonar pulse to the structures, generating a larger noise-free void in which fishes can be quantified, and compensating for the redundant volume of water taken up by the near-field zone in which fishes cannot be fully ensonified. Imaging sonars may ultimately play a key role in remote sensing of marine habitats and assemblages, particularly at lower frequencies of greater range (e.g., 10 m at 0.75, 1.2, and 2.1 MHz in this study).

Finally, geometric scattering of the high frequency imaging sonar pulse may have resulted in double counting of fish targets. Geometric scattering occurs due to the very small wavelengths of high frequency beam arrays hitting relatively large objects such as fishes, causing the beams to variably scatter off different body parts of contrasting density, such as bones, muscle tissue, and swimbladders (Foote, 1980; Simmons and MacLennan, 2005). The smaller the wavelength, the greater the capacity to discriminate internal components of fishes. On imaging sonar displays, this can result in segmented targets that may objectively appear as two or more discrete individuals. To mitigate inflation of fish counts, the data processor (E.C.P. Sibley) spent several hours identifying and recognising different forms of geometric scattering and used continuous footage where necessary to determine the true or false presence of multiple targets in instances of scattering. Prior to making manual counts of fishes, this study advocates training of observers in identifying these sources of error, particularly in being able to consistently discriminate fishes from non-fish objects (Jones et al., 2021; Keefer et al., 2017). Differences in the experience of observers in processing imaging sonar footage may result in disparities in fish counts that ultimately impact estimates of fish density (Keefer et al., 2017; Lagarde et al., 2020; Petreman et al., 2014).

4.2. Fish density quantification & instrument comparison

Fish assemblages were dominated by small, site-attached species, most notably West Australian pullers (*Chromis westaustralis*) and western king wrasse (*Coris auricularis*) that accounted for between 37% and 74% and 21–59% of all fishes observed at each frequency in the optic still frames respectively (Table 2). The colour of *C. westaustralis* typically varies from dark teal to olive green – a spectrum near identical to that of the algal growth that covered most of the lower depth strata of the towers. Subsequently, *C. westaustralis* in close proximity to the towers were often camouflaged from optic detection by the towers (Fig. 2c). Similarly, *C. auricularis* are predominantly bleached white in colour. As such, individuals near the sandy seabed were often inconspicuous, and therefore were likely underrepresented in optic estimates of fish density. In contrast, the capacity of imaging sonar to detect physical objects independent of distinguishing features used in optic surveys, such as colour, likely underpinned higher sonar fish densities (particularly when coinciding with high densities of *C. westaustralis* and *C. auricularis*). Here, the data processor noted that *C. westaustralis* and *C. auricularis* could infrequently be discriminated from the towers and seabed respectively by fine-scale morphological features such as eye colour, that contrasted with the background. However, use of an HD optical camera still was not adequate to consistently resolve such characteristics. Given the high motility of *C. westaustralis* and *C. auricularis*, using continuous optic footage may help to discriminate similarly camouflaged fishes in future studies, provided that the background habitat is not homogeneous in colour.

Previous studies of small, highly site-attached camouflaged taxa using ROVs have considered underrepresentation of such taxa in subsequent optic analyses due to the limited proximity of the ROV to physical habitat due to entanglement and damage risk (Ajemian et al., 2015; Wetz et al., 2020). Here, this study demonstrates that imaging sonar can enumerate fishes irrespective of both degree of camouflage and distance to hard structure habitat. For the latter, the distance gradings and measurement tool on the Oculus Viewpoint software allow the distance between fish targets and habitat to be quantified, generating empirical habitat associations that may prove valuable in future ecological studies. Additionally, the ability of imaging sonar to consistently detect and quantify the abundant and diverse small-bodied species at the Rottnest fish towers reinforces the ability of high-frequency acoustics to capture small fishes (Becker et al., 2016, 2013; Egg et al., 2018; Kimball et al., 2010; Mueller et al., 2006). Imaging sonar may particularly outperform some optical cameras in this capacity: as reported by Egg et al. (2018), the minimum size detection threshold of an Adaptive Resolution Imaging Sonar (ARIS) operating at 3 MHz was 10 cm, versus 15 cm for an HD GoPro Hero 4. Indeed, as described by Kimball et al. (2010) using a 1.8 MHz DIDSON, objects as small as 2 cm can be consistently detected by imaging sonar. Moreover, underestimation of small targets using imaging sonar at greater range due to decreasing resolution is only apparent beyond 20 m (summarised in Wei et al., 2022), significantly greater than the sampling ranges in this study. Nonetheless, this study advises that the accuracy of imaging sonar estimates of fish density may be impacted at ranges exceeding 20 m.

The variation in fish density observed across imaging sonar frequencies in this study is not considered to be informative. Differences in the wavelengths of all four frequencies are too finite relative to the size

of the fishes surveyed to incur variations in fish density. Higher fish density at 3 MHz is instead likely a product of covariance between frequency and the tower surveyed (either north or south). Only the north tower was surveyed at 3 MHz, with the south tower surveyed at 0.75, 1.2 and 2.1 MHz. Accordingly, ecological factors operating on different spatial and temporal scales between the towers probably generated the higher fish density at the 3 MHz north tower survey. These factors may include variable proximity to source habitat or vectors of dispersal, such as the Leeuwin current (Caputi et al., 1996; Hutchins and Pearce, 1994), or differences in tidal regimes. To negate the influence of inter-habitat differences, future studies comparing imaging sonar fish densities across multiple frequencies should survey just one habitat, or apportion sampling effort equally by method (e.g., frequency) among different habitats. At equivalent fish abundance and consistent range, lower densities may be expected at higher frequencies. As reported by Cotter and Polagye (2020), detections of marine fauna at 2.25 MHz were lower than at 0.72 MHz due to attenuation of returning echoes by entrained air that shadowed targets at higher frequencies (see also Melvin and Cochrane, 2015). However, that study took place at a tidal channel with high water turbulence, and the magnitude of acoustic signal attenuation is likely lower in calmer waters, such as those around the Rottnest fish towers. Inconsistency in fish densities between the frequencies used to survey the south tower also indicate intra-habitat differences, a possible product of temporal variation in fish assemblage abundance and composition, and unlikely to be indicative of instrumental inconsistencies (such as wavelength variation) across 0.75, 1.2, and 2.1 MHz.

The fish densities quantified by both imaging sonar and the optical camera may have been adversely influenced on occasions where the ROV was not fully horizontal. Although conditions were relatively calm during the survey period, instances of stronger current caused the ROV to pitch and roll beyond an orthogonal axis. This may have falsely altered the sampling volumes of the imaging sonar and camera, in turn affecting fish density calculations. Furthermore, downward pitching of the ROV occasionally resulted in acoustic and optic obstruction by the seabed. Though sonar fish densities were not lower in frames with seabed interference (despite some instances of fish masking), and seabed was accounted for in optic volume calculations, future studies should be aware of potential variation in fish densities resulting from inconsistent ROV orientation. Finally, an additional factor that likely influenced optic volumes was lens barrel distortion caused by the dome port of the camera used in this study. Lens distortion requires 3-D image analyses to correct (Davies, 2018), which was beyond the scope of this study, though the accuracy of future estimates of fish density would be improved by remedying various causes of optic instrument distortion. Three-dimensional (3-D) image analyses also extend to stereo-video, a technique widely used to derive fish length estimates using optics (Harvey et al., 2002). Future comparisons between imaging sonar and optics may look to employ a stereo-video complex for comparison of length estimates from both instruments (Cook et al., 2019), which was not possible with the single camera system used here. Stereo-video systems would also provide information on the position of fishes in the water column; imaging sonar compresses the detection of objects in 3-D space into two dimensions for display (Martignac et al., 2015). The impact of this compression is here considered negligible given that imaging sonar did not quantify lower fish densities than optics, suggesting that there were few or no fishes in the same vertical plane that would otherwise obstruct one another on the imaging sonar display. However, if arrangement of fishes in 3-D space is desirable, or if the target assemblage is very dense (e.g., schooling fishes) such that obstruction of fishes in a two-dimensional display is likely, this study suggests also implementing a calibrated, multi-camera optical instrument to determine the orientation of fishes detected by imaging sonar. Alternatively, rotating the imaging sonar could ensonify fishes in the vertical dimension (Boswell et al., 2019), whilst 3-D modelling and reconstruction of imaging sonar footage is also possible (Jing et al., 2018).

5. Conclusion

This study reports that imaging sonar enumerated higher fish densities than an optical camera at three out of four frequencies tested (0.75, 1.2, and 3 MHz). This finding encourages the deployment of imaging sonars for surveying the fish assemblages of other complex hard substrate habitats, including other artificial habitats like rigs-to-reefs (Plumlee et al., 2020), and biogenic reefs (Griffin et al., 2020). Most notably, imaging sonar outperformed optics in the detection of small, camouflaged, site-attached fishes that dominated the assemblages surveyed in this study. Further use of imaging sonar to enumerate size-diverse and speciose assemblages across different habitats, particularly in comparison with simultaneous optical methods, will provide valuable indication of the wider potential of sonars in fish surveys. Crucially, this study also identified several limitations of imaging sonar in addition to the broader constraints of acoustic instruments that may constrain the use of sonar for future investigations, many of which can be remedied by simultaneous use of optics (Table 3). The capacity of imaging sonar to enumerate higher fish densities than optics consolidates both its broader application in marine life assessments, particularly as a complimentary tool to optics, as well as its use as a substitute for optics in instances of low-light.

Ethics statement

The animal study for the collection of field data was reviewed and approved by the Curtin University Animal Ethics Committee (ARE 2021 18).

Funding

This research project was funded by Chevron through a research grant to Curtin University under the Western Australian Energy Research Alliance (AES 17-P2TD-151-A1) and its Anchor Partnership with the UK National Decommissioning Centre. We also acknowledge in-kind support from Net Zero Technology Centre and the University of Aberdeen through their partnership with the UK National Decommissioning Centre.

CRediT authorship contribution statement

Edward C.P. Sibley: Conceptualisation, Data curation, Formal analysis, Investigation, Methodology, Visualization, Writing – original draft, Writing – review & editing. **Travis S. Elsdon:** Conceptualisation, Funding acquisition, Formal analysis, Methodology, Project administration, Resources, Supervision, Writing – review & editing. **Michael J. Marnane:** Conceptualisation, Funding acquisition, Methodology, Project administration, Resources, Supervision, Writing – review & editing. **Alethea S. Madgett:** Project administration, Supervision, Writing – review & editing. **Euan S. Harvey:** Conceptualisation, Data curation, Investigation, Methodology, Resources, Writing – review & editing. **Thomas Cornulier**: Formal analysis, Writing – review & editing. **Damon Driessen:** Data curation, Investigation. **Paul G. Fernandes:** Conceptualisation, Formal analysis, Methodology, Project administration, Supervision, Visualisation, Writing – review & editing.

Declaration of Competing Interest

The authors declare that they have no known competing financial interests or personal relationships that could have appeared to influence the work reported in this paper. This research was funded by Chevron through a research grant to Curtin University and Anchor Partnership with the National Decommissioning Centre. E. S. Harvey received funding for this, and other research projects from Chevron. M. J. Marnane and T. S. Elsdon work for Chevron and are interested in understanding the potential ecological and socio-economic value of artificial

structures in the marine environment. All the views expressed within the paper are those of the authors and have been uninfluenced by their affiliations.

Data Availability

Data will be made available on request.

Acknowledgements

We acknowledge Kevin Holden from DeepVision Subsea, Ben Saunders and Iain Parnum for the collection of video and acoustic imagery. We thank Tony Scarangella for the provision and skippering of the research vessel, and Matthew Allen at Subcon for provision of schematics of the Rottnest fish towers.

Appendix A. Supporting information

Supplementary data associated with this article can be found in the online version at doi:10.1016/j.fishres.2023.106720.

References

Able, K.W., Grothues, T.M., Kemp, I.M., 2013. Fine-scale distribution of pelagic fishes relative to a large urban pier. Mar. Ecol. Prog. Ser. 476, 185–198.
Accola, K.L., Horne, J.K., Cordell, J.R., Toft, J.D., 2022. Acoustic characterization of juvenile Pacific salmon distributions along an eco-engineered seawall. Mar. Ecol. Prog. Ser. 682, 207–220.
Ajemian, M.J., Wetz, J.J., Shipley-Lozano, B., Stunz, G.W., 2015. Rapid assessment of fish communities on submerged oil and gas platform reefs using remotely operated vehicles. Fish. Res. 167, 143–155.
Artero, C., Marchetti, S., Bauer, E., Viala, C., Noel, C., Koenig, C.C., Berzins, R., Lampert, L., 2021. High-resolution acoustic cameras provide direct and efficient assessments of large demersal fish populations in extremely turbid waters. Appl. Sci. 11, 1899.
Becker, A., Suthers, I.M., 2014. Predator driven diel variation in abundance and behaviour of fish in deep and shallow habitats of an estuary. Estuar. Coast. Shelf Sci. 144, 82–88.
Becker, A., Whitfield, A., Cowley, P., Järnegren, J., Næsje, T., 2011. An assessment of the size structure, distribution and behaviour of fish populations within a temporarily closed estuary using dual frequency identification sonar (DIDSON). J. Fish. Biol. 79, 761–775.
Becker, A., Whitfield, A.K., Cowley, P.D., Järnegren, J., Næsje, T.F., 2013. Potential effects of artificial light associated with anthropogenic infrastructure on the abundance and foraging behaviour of estuary-associated fishes. J. Appl. Ecol. 50, 43–50.
Becker, A., Holland, M., Smith, J.A., Suthers, I.M., 2016. Fish movement through an estuary mouth is related to tidal flow. Estuaries Coasts 39, 1199–1207.
Bollinger, M.A., Kline, R.J., 2017. Validating sidescan sonar as a fish survey tool over artificial reefs. J. Coast. Res 33, 1397–1407.
Bolser, D.G., Egerton, J.P., Grüss, A., Loughran, T., Beyea, T., McCain, K., Erisman, B.E., 2020. Environmental and structural drivers of fish distributions among petroleum platforms across the US Gulf of Mexico. Mar. Coast. Fish 12, 142–163.
Bond, M.E., Babcock, E.A., Pikitch, E.K., Abercrombie, D.L., Lamb, N.F., Chapman, D.D., 2012. Reef sharks exhibit site-fidelity and higher relative abundance in marine reserves on the mesoamerican barrier reef. PLoS One 7, e32983. https://doi.org/10.1371/journal.pone.0032983.
Boswell, K.M., Wells, R., Cowan Jr, J.H., Wilson, C.A., 2010. Biomass, density, and size distributions of fishes associated with a large-scale artificial reef complex in the Gulf of Mexico. Bull. Mar. Sci. 86, 879–889.
Boswell, K.M., Kimball, M.E., Rieucau, G., Martin, J.G., Jacques, D.A., Correa, D., Allen, D.M., 2019. Tidal stage mediates periodic asynchrony between predator and prey nekton in salt marsh creeks. Estuaries Coasts 42, 1342–1352.
Brehmer, P., Do Chi, T., Mouillot, D., 2006. Amphidromous fish school migration revealed by combining fixed sonar monitoring (horizontal beaming) with fishing data. J. Exp. Mar. Biol. Ecol. 334, 139–150.
Capoccioni, F., Leone, C., Pulcini, D., Cecchetti, M., Rossi, A., Ciccotti, E., 2019. Fish movements and schooling behavior across the tidal channel in a Mediterranean coastal lagoon: an automated approach using acoustic imaging. Fish. Res. 219, 105318.
Caputi, N., Fletcher, W., Pearce, A., Chubb, C., 1996. Effect of the Leeuwin Current on the recruitment of fish and invertebrates along the Western Australian coast. Mar. Freshw. Res. 47, 147–155.
Cook, D., Middlemiss, K., Jaksons, P., Davison, W., Jerrett, A., 2019. Validation of fish length estimations from a high frequency multi-beam sonar (ARIS) and its utilisation as a field-based measurement technique. Fish. Res. 218, 59–68.
Cotter, E., Polagye, B., 2020. Detection and classification capabilities of two multibeam sonars. Limnol. Oceanogr. Methods 18, 673–680.
Davies, E.R., 2018. Image transformations and camera calibration. In: Computer Vision. Elsevier, pp. 585–610. https://doi.org/10.1016/B978-0-12-809284-2.00019-8.
Dickens, L.C., Goatley, C.H., Tanner, J.K., Bellwood, D.R., 2011. Quantifying relative diver effects in underwater visual censuses. PloS One 6, e18965.
Dunlop, K.M., Marian Scott, E., Parsons, D., Bailey, D.M., 2015. Do agonistic behaviours bias baited remote underwater video surveys of fish. Mar. Ecol. 36, 810–818.
Egg, L., Mueller, M., Pander, J., Knott, J., Geist, J., 2017. Improving European Silver Eel (Anguilla anguilla) downstream migration by undershot sluice gate management at a small-scale hydropower plant. Ecol. Eng. 106, 349–357.
Egg, L., Pander, J., Mueller, M., Geist, J., 2018. Comparison of sonar-, camera-and net-based methods in detecting riverine fish-movement patterns. Mar. Freshw. Res. 69, 1905–1912.
Eggleston, M.R., Milne, S.W., Ramsay, M., Kowalski, K.P., 2020. Improved fish counting method accurately quantifies high-density fish movement in dual-frequency identification sonar data files from a coastal wetland environment. North Am. J. Fish. Manag. 40, 883–892.
Faulkner, A.V., Maxwell, S.L., 2020. Adult sockeye salmon assessment in a tidal, turbid river: a comparison of sonar and test fishing methods. North Am. J. Fish. Manag 40, 852–864.
Fernandes, P.G., Copland, P., Garcia, R., Nicosevici, T., Scoulding, B., 2016. Additional evidence for fisheries acoustics: small cameras and angling gear provide tilt angle distributions and other relevant data for mackerel surveys. ICES J. Mar. Sci. 73, 2009–2019.
Foote, K.G., 1980. Importance of the swimbladder in acoustic scattering by fish: a comparison of gadoid and mackerel target strengths. J. Acoust. Soc. Am. 67, 2084–2089.
Grabowski, T.B., Boswell, K.M., McAdam, B.J., Wells, R.D., Marteinsdóttir, G., 2012. Characterization of Atlantic cod spawning habitat and behavior in Icelandic coastal waters. PLoS One 7, e51321.
Griffin, R.A., Jones, R.E., Lough, N.E., Lindenbaum, C.P., Alvarez, M.C., Clark, K.A., Griffiths, J.D., Clabburn, P.A., 2020. Effectiveness of acoustic cameras as tools for assessing biogenic structures formed by Sabellaria in highly turbid environments. Aquat. Conserv. Mar. Freshw. Ecosyst. 30, 1121–1136.
Han, C.-H., Uye, S.-I., 2009. Quantification of the abundance and distribution of the common jellyfish Aurelia aurita sl with a Dual-frequency IDentification SONar (DIDSON). J. Plankton Res. 31, 805–814.
Handegard, N.O., Boswell, K.M., Ioannou, C.C., Leblanc, S.P., Tjøstheim, D.B., Couzin, I. D., 2012. The dynamics of coordinated group hunting and collective information transfer among schooling prey. Curr. Biol. 22, 1213–1217.
Harvey, E., Shortis, M., Stadler, M., Cappo, M., 2002. A comparison of the accuracy and precision of measurements from single and stereo-video systems. Mar. Technol. Soc. J. 36, 38–49.
Holmes, J.A., Cronkite, G.M., Enzenhofer, H.J., Mulligan, T.J., 2006. Accuracy and precision of fish-count data from a "dual-frequency identification sonar"(DIDSON) imaging system. ICES J. Mar. Sci. 63, 543–555.
Hutchins, J., Pearce, A., 1994. Influence of the Leeuwin Current on recruitment of tropical reef fishes at Rottnest Island, Western Australia. Bull. Mar. Sci. 54, 245–255.
Jing, D., Han, J., Zhang, J., 2018. A method to track targets in three-dimensional space using an imaging sonar. Sensors 18, 1992.
Jones, R.E., Griffin, R.A., Unsworth, R.K., 2021. Adaptive Resolution Imaging Sonar (ARIS) as a tool for marine fish identification. Fish. Res. 243, 106092.
Keefer, M.L., Caudill, C.C., Johnson, E.L., Clabough, T.S., Boggs, C.T., Johnson, P.N., Nagy, W.T., 2017. Inter-observer bias in fish classification and enumeration using dual-frequency identification sonar (didson): A pacific lamprey case study. Northwest Sci. 91, 41–53.
Kimball, M.E., Rozas, L.P., Boswell, K.M., Cowan Jr, J.H., 2010. Evaluating the effect of slot size and environmental variables on the passage of estuarine nekton through a water control structure. J. Exp. Mar. Biol. Ecol. 395, 181–190.
Lagarde, R., Peyre, J., Amilhat, E., Mercader, M., Prellwitz, F., Simon, G., Faliex, E., 2020. In situ evaluation of European eel counts and length estimates accuracy from an acoustic camera (ARIS). Knowl. Manag. Aquat. Ecosyst. 44.
Langkau, M., Clavé, D., Schmidt, M., Borcherding, J., 2016. Spawning behaviour of Allis shad Alosa alosa: new insights based on imaging sonar data. J. Fish. Biol. 88, 2263–2274.
Lankowicz, K.M., Bi, H., Liang, D., Fan, C., 2020. Sonar imaging surveys fill data gaps in forage fish populations in shallow estuarine tributaries. Fish. Res. 226, 105520.
Lorance, P., Trenkel, V.M., 2006. Variability in natural behaviour, and observed reactions to an ROV, by mid-slope fish species. J. Exp. Mar. Biol. Ecol. 332, 106–119.
MacLennan, D.N., Holliday, D., 1996. Fisheries and plankton acoustics: past, present, and future. ICES J. Mar. Sci. 53, 513–516.
Martignac, F., Daroux, A., Bagliniere, J., Ombredane, D., Guillard, J., 2015. The use of acoustic cameras in shallow waters: new hydroacoustic tools for monitoring migratory fish population. A review of DIDSON technology. Fish Fish. 16, 486–510.
McLean, D., Taylor, M., Partridge, J., Gibbons, B., Langlois, T., Malseed, B., Smith, L., Bond, T., 2018. Fish and habitats on wellhead infrastructure on the north west shelf of Western Australia. Cont. Shelf Res. 164, 10–27.
Melvin, G.D., Cochrane, N.A., 2015. Multibeam acoustic detection of fish and water column targets at high-flow sites. Estuaries Coasts 38, 227–240.
Moursund, R.A., Carlson, T.J., Peters, R.D., 2003. A fisheries application of a dual-frequency identification sonar acoustic camera. ICES J. Mar. Sci. 60, 678–683.
Mueller, R.P., Brown, R.S., Hop, H., Moulton, L., 2006. Video and acoustic camera techniques for studying fish under ice: a review and comparison. Rev. Fish. Biol. Fish. 16, 213–226.
Munnelly, R.T., Reeves, D.B., Chesney, E.J., Baltz, D.M., Marx, B.D., 2019. Habitat suitability for oil and gas platform-associated fishes in Louisiana's nearshore waters. Mar. Ecol. Prog. Ser. 608, 199–219.

Petreman, I.C., Jones, N.E., Milne, S.W., 2014. Observer bias and subsampling efficiencies for estimating the number of migrating fish in rivers using Dual-frequency IDentification SONar (DIDSON). Fish. Res. 155, 160–167.
Plumlee, J.D., Dance, K.M., Dance, M.A., Rooker, J.R., TinHan, T.C., Shipley, J.B., Wells, R., 2020. Fish assemblages associated with artificial reefs assessed using multiple gear types in the northwest Gulf of Mexico. Bull. Mar. Sci. 96, 655–678.
Rieucau, G., Holmin, A.J., Castillo, J.C., Couzin, I.D., Handegard, N.O., 2016. School level structural and dynamic adjustments to risk promote information transfer and collective evasion in herring. Anim. Behav. 117, 69–78.
Rodriguez-Pinto, I.I., Rieucau, G., Handegard, N.O., Kimball, M.E., Boswell, K.M., 2022. Anthropogenic Marsh Impoundments Alter Collective Tendency in Schooling Fish. Estuaries Coasts 45, 856–865.
Samoilys, M.A., Carlos, G., 2000. Determining methods of underwater visual census for estimating the abundance of coral reef fishes. Environ. Biol. Fishes 57, 289–304.
Shahrestani, S., Bi, H., Lyubchich, V., Boswell, K.M., 2017. Detecting a nearshore fish parade using the adaptive resolution imaging sonar (ARIS): An automated procedure for data analysis. Fish. Res. 191, 190–199.
Simmons, E., MacLennan, D., 2005. Fisheries acoustics. Theory Pract, second ed. Publ. Blackwell Sci.
Staines, G.J., Mueller, R.P., Seitz, A.C., Evans, M.D., O'Byrne, P.W., Wosnik, M., 2022. Capabilities of an acoustic camera to inform fish collision risk with current energy converter turbines. J. Mar. Sci. Eng. 10, 483.
Stanley, D.R., Wilson, C.A., 1997. Seasonal and spatial variation in the abundance and size distribution of fishes associated with a petroleum platform in the northern Gulf of Mexico. Can. J. Fish. Aquat. Sci. 54, 1166–1176.
Stanley, D.R., Wilson, C.A., 2000. Variation in the density and species composition of fishes associated with three petroleum platforms using dual beam hydroacoustics. Fish. Res. 47, 161–172.
Stoner, A.W., Ryer, C.H., Parker, S.J., Auster, P.J., Wakefield, W.W., 2008. Evaluating the role of fish behavior in surveys conducted with underwater vehicles. Can. J. Fish. Aquat. Sci. 65, 1230–1243.
Team, R.C., 2013. R: A language and environment for statistical computing. R Foundation for Statistical Computing, Vienna, Austria. Httpwww R-Proj. Org.
Tessier, E., Chabanet, P., Pothin, K., Soria, M., Lasserre, G., 2005. Visual censuses of tropical fish aggregations on artificial reefs: slate versus video recording techniques. J. Exp. Mar. Biol. Ecol. 315, 17–30.
Van Hal, R., Griffioen, A., Van Keeken, O., 2017. Changes in fish communities on a small spatial scale, an effect of increased habitat complexity by an offshore wind farm. Mar. Environ. Res. 126, 26–36.
Viehman, H.A., Zydlewski, G.B., 2015. Fish interactions with a commercial-scale tidal energy device in the natural environment. Estuaries Coasts 38, 241–252.
Wei, Y., Duan, Y., An, D., 2022. Monitoring fish using imaging sonar: capacity, challenges and future perspective. Fish Fish.
Wetz, J.J., Ajemian, M.J., Shipley, B., Stunz, G.W., 2020. An assessment of two visual survey methods for documenting fish community structure on artificial platform reefs in the Gulf of Mexico. Fish. Res. 225, 105492.
Willis, T.J., Babcock, R.C., 2000. A baited underwater video system for the determination of relative density of carnivorous reef fish. Mar. Freshw. Res 51, 755–763.
Wood, S., Wood, M.S., 2015. Package 'mgcv'. R. Package Version 1, 729.